# 論文の内容の要旨

## 論文題目 Controlling the electronic states at the $LaAlO_3/SrTiO_3$ heterointerface

（$LaAlO_3/SrTiO_3$ ヘテロ界面における電子状態の制御）

氏　　名　　　　　　　　細田　雅之

### Introduction

Interfaces between perovskite oxides have drawn much interest in pursuit of novel functionalities. The enticement of this system comes not only from the wide-ranging electronic properties of the parental bulk, but from the fact that they have common (quasi-)cubic structure with a similar lattice constant. This means that high-quality epitaxial interfaces are obtained with a wide variety of combinations of functional oxides, opening the way to pursue new devices by design. The conductivity at the $LaAlO_3/SrTiO_3$ (LAO/STO) heterointerface is a striking example of an emergent state at a perovskite heterointerface. This interface shows high mobility electron transport although both constituent layers are band insulators.[1] Various exotic phenomena, including two-dimensional superconductivity, two-dimensional Shubnikov-de Haas oscillations and magnetism are observed at low temperatures. The emergence of these phenomena is regarded to be intimately linked to the carrier distribution and the carrier density $n$, after several methods have been found to be important in determining $n$ and the electronic properties, such as a variation of the growth conditions, thickness of the LAO layer, surface adsorbates and so on. In order to further push this system to its limits, a scalable and clean way of tuning the carrier density is crucial, in respect of gaining both fundamental understanding of the electron correlations and for device applications. This thesis presents two strategies to modulate the carrier density at the LAO/STO interface: delta-doping and electrostatic modulation.

### Delta-doping the LAO/STO interface

In order to achieve scalable carrier density modulation while maintaining high-mobility transport, epitaxial $LaTiO_3$ (LTO) layers were employed as dopant layers. LTO is a perovskite Mott insulator well lattice-matched to STO, known to donate electrons when embedded in STO heterostructures.[2, 3] This structure maintains the consistency of the conduction band originated from Ti 3$d$-electrons and minimizes unwanted scattering centers which have been a problem faced by using relatively lightly-doped conducting layers attempted so far.[4, 5] All samples with the epitaxial structure LAO ($x$ uc) /LTO ($y$ uc)/STO were grown by pulsed laser deposition (PLD), by depositing an LTO layer with thickness of $y$ unit cells (uc) on a single crystalline STO with $TiO_2$ {001}-termination, then depositing an $x$-uc-thick LAO [Fig. 1(a) inset]. Focusing on the $x = 3$ series, the temperature dependence of the sheet resistances is shown in Fig.

1(a) for typical samples with $(x, y) = (3, 0.25)$, (3, 0.5), (3, 1) and (3, 3). All show a monotonically decreasing sheet resistance down to ~ 100 Ω/sq. at the temperature $T = 2$ K. A nonlinear Hall resistance vs. magnetic field was observed for all samples, which could be well fitted using a two-carrier model where two parallel carrier layers with different carrier densities, $n_1$ and $n_2$, and mobilities, $\mu_1$ and $\mu_2$, respectively, are assumed, which we ascribe to the spatial variation of the carrier density in the depth direction [3]. $n_{tot} = n_1+n_2$ and $\mu_{ave} = (n_1\mu_1+n_2\mu_2) / (n_1+n_2)$ as well as $n_2$ and $\mu_2$ are shown for a various $y$ in Fig. 1(b). $n_{tot}$ rapidly increased with small $y$, reaching values of $n_{tot}$ ~ $1\times10^{14}$ $cm^{-2}$, before saturating above $y$ = 0.5 uc. Combining the systematic variation of $n_{tot}$ and conductivity with variation of the $(x, y)$ shown in Fig. 2, we could determine the role of the LTO as a dopant layer in this system. In regard to the polar discontinuity between LAO and STO {001}, one of the intriguing possible origins of the Q2DEG in this system, we can consider LTO simply as a polar layer akin to LAO, with alternating {001} layers of $(La^{3+}O^{2-})^+$ and $(Ti^{3+}O_2^{4-})^-$ in the ionic limit. This assignment can be ruled out however, since we would expect that conductivity is observed for $x + y \gtrsim 3$ uc, leading to a phase boundary that follows the dashed line in Fig. 2, which is in disagreement with the data. Instead we can consider LTO acting as a dopant layer due to the constituent $Ti^{3+}$ ions, which form $3d^1$ electrons that can migrate into the empty $3d^0$ orbitals in the STO and make $n$ significantly higher than for typical LAO/STO samples without LTO.

Next we investigated the effect of the LTO insertion on the field-effect response using a gate contact on the back side of the STO substrate. The gate voltage $V_G$ dependences of the carrier density and mobility for a $(x, y) = (3, 0.25)$ sample at $T = 2$ K are shown in Fig. 3. The Hall non-linearity was observed for positive gate voltages. $n_{tot}$ shown here is the total density determined after the two-carrier analyses. For this (3, 0.25) sample, a change from $n_{tot} = 4.9\times10^{13}$ $cm^{-2}$ at $V_G = 0$ V could be suppressed down to $2.4\times10^{13}$ $cm^{-2}$ at $V_G = -100$ V, in good agreement with the value expected from a simple capacitor model employing a STO dielectric constant $\varepsilon_{STO}$ =

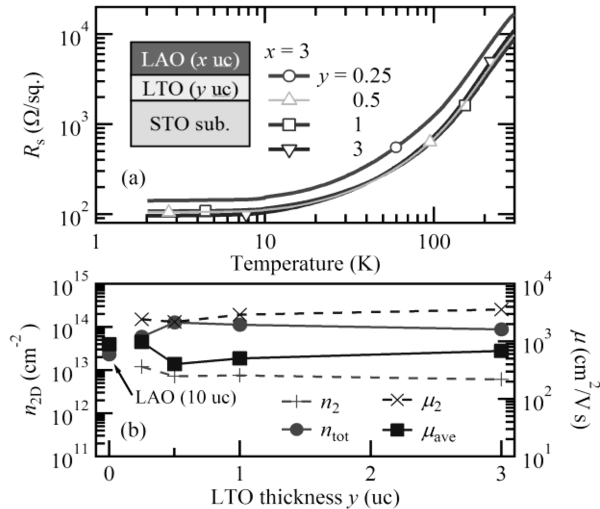


Fig. 1. (a) Temperature dependence of the sheet resistance and (b) the Hall carrier density and Hall mobility for representative samples with a fixed LAO thickness of 3 uc. The inset of (a) shows a schematic of the structure of the samples. Data for LAO (10 uc)/STO are also plotted at $y = 0$ for reference. Lines are guides.

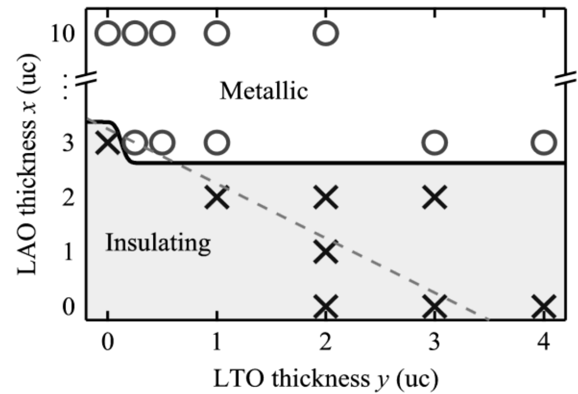


Fig. 2. Conductivity variation with different LAO and LTO thicknesses. Circles represent metallic conductivity, and crosses insulating behavior. Observed phase boundary is indicated with a solid line. Dashed line shows the predicted phase boundary $x + y \gtrsim 3$ uc if the LTO is assumed as a simple polar stack.

20000, and substrate thickness 0.5 mm, as depicted as a dashed gray line in Fig. 3. These data were quite distinct to those of LAO/STO where a relatively small modulation of $n$ and large change in $\mu$ is observed. For $V_G > 0$, both $n_1$ and $n_2$ increased, suggesting spreading of the carrier distribution into the depth of the substrate, where the mobility is relatively enhanced.

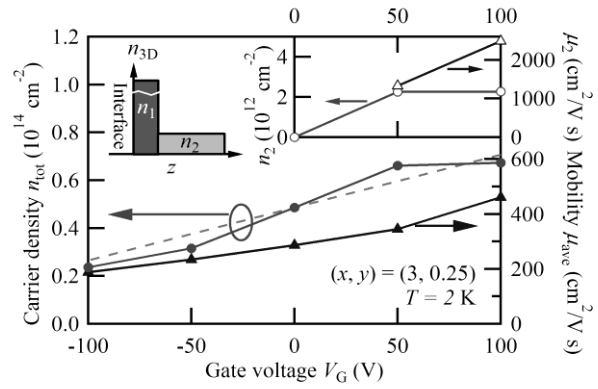


Fig. 3. $V_G$ dependence of the $n_{tot}$ and $\mu_{ave}$ of the LAO (3 uc)/LTO (0.25 uc)/STO sample extracted from a two-carrier fit at $T$ = 2 K. Dashed gray line shows the slope expected from the capacitance between the interface and gate contact; other lines are guides.

## Electric field carrier modulation via top gate

The field-effect transistors (FETs) with Hall-bar structure were made on LAO/STO samples with various LAO thickness using standard optical photolithography and a gold top gate [Fig. 4(a), (b)]. Room temperature transport characteristics of the sample with 7-uc-thick LAO are shown in Fig. 4(c). The drain-source current $I_D$ was clearly modulated by the top-gate voltage $V_{GS}$ in a region where $I_D$ is independent of $V_{DS}$, indicating the drain-source channel is pinched off at the saturated current $I_{DSS}$, similar to the characteristics derived from the commonly known gradual channel model where $n$ is ideally controlled by $V_{GS}$ and $\mu$ is assumed to stay constant. $I_{DSS}$ showed the typical quadratic dependence on $V_{GS}$ above the threshold voltage $V_{TH}$ [Fig .4(d)]. At a lower temperature, modulation of $n$ by $V_G$ was demonstrated by Hall measurements in a 16-uc-thick LAO sample [Fig. 5]. Interestingly, $\mu$ showed a clear increase with decreasing $n$, which is the opposite tendency to back gate modulation [6]. This could be understood in two ways; one is that population of electrons at the immediate interface, which have lower mobility due to interfacial scattering potential, was reduced by negative $V_{GS}$, resulting in increase of the average mobility. The other is that the resulting three-dimensional electron density is smaller with smaller $V_{GS}$, and the reduced electron-electron interactions resulted in a higher mobility. In reality both of these effects are likely to occur simultaneously, and the potential significance here is that

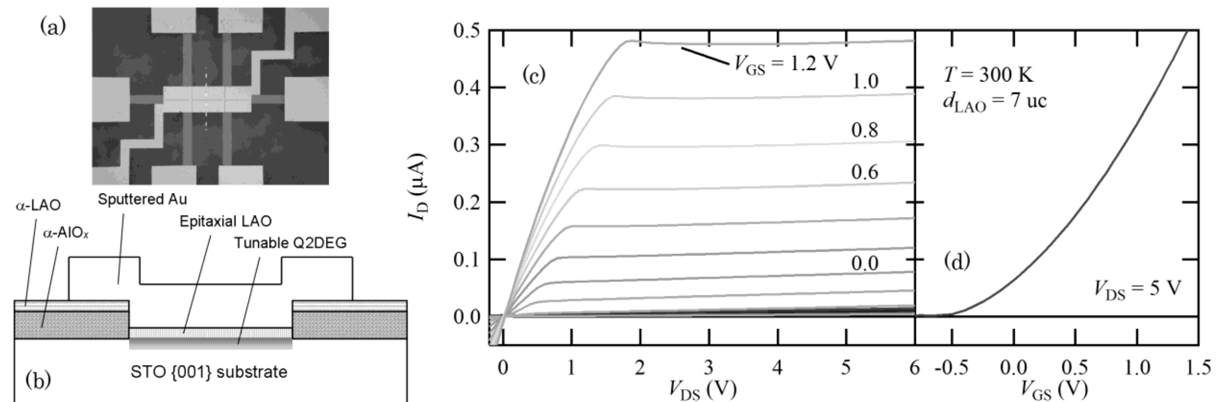


Fig. 4. The FET structure. (a) Top view picture and (b) cross-section view along the dotted line in (a). α denotes amorphous. (c) Room temperature $I_D$-$V_{DS}$ curves of the FET device with 7-uc-thick LAO, taken with the 0.2 V steps of $V_{GS}$ showed a wide-ranged saturation region. (d) The transfer curve of the same device showed an ideal quadratic behavior of $I_D$ when $V_{GS}$ was increased over $V_{TH}$ ~ -0.5 V.

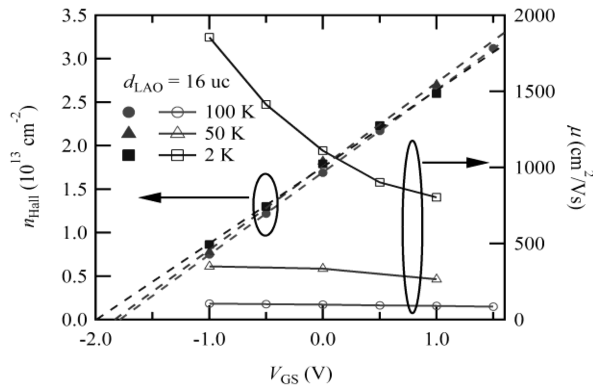


Fig. 5. $n$ and $\mu$ vs. $V_{GS}$ at lower temperature. $V_{TH}$ stayed around -1.8 V at the range of temperature as indicated with fitted dashed lines, suggesting robust $n$ modulation is achieved. Mobility enhancement is clear. Solid lines are guides.

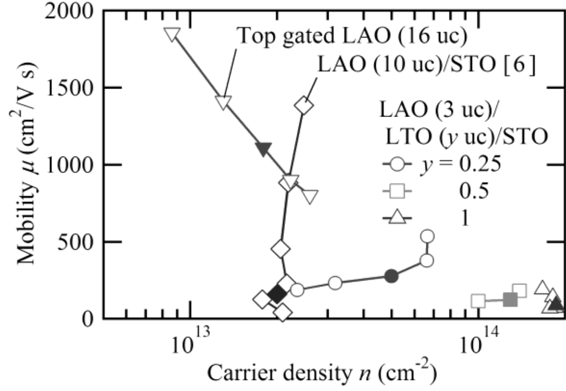


Fig. 6. $n$ and $\mu$ achieved in the current study. Solid marks show data ungated, while open ones are their variation by applying top/back gate voltage to a single sample. All data were taken at $T$ = 2 K.

systematic $n$ suppression achieved by top gate voltage at all temperature range, providing access to a regime with both smaller carrier density and less disorder, where other methods have experienced difficulties in approaching.

## Conclusion

We have demonstrated carrier tuning at the LAO/STO interfaces by delta-doping and top gating the interfaces. By inserting a LTO layer, the carrier density of the LAO/STO interfaces could be increased accordingly to the thickness of the LTO layer, and further modulated by electric field applied to the back gate. Top gating was found to be a robust way in modulating carrier density, showing ideal device characteristics at room temperature, and also clear $n$ modulation at all temperatures. The variation of the electron density and accompanying mobility change of several samples studied in this Thesis at $T$ = 2 K are shown in Fig. 6. The open symbols connected with a line show the modulation by the top/back gate in a single sample whose ungated data are indicated with solid symbols. These data suggest that a wide-range modulation of the carrier density from $8\times10^{13}$ to $2\times10^{14}$ cm$^{-2}$ was achieved by combining the methods established in this Thesis. One intriguing perspective to mention is that top and back gating show opposite trends in the mobility modulation, suggesting that by applying both simultaneously, completely independent control of the carrier density and mobility, or carrier distribution can be achieved, providing a powerful tool to investigate the nature of the LAO/STO interface.

## References

[1] A. Ohtomo and H. Y. Hwang, Nature 427, 423 (2004).

[2] A. Ohtomo *et al.*, Nature 419, 378 (2002).

[3] R. Ohtsuka *et al.*, Appl. Phys. Lett. 96, 192111 (2010).

[4] T. Fix *et al.*, Appl. Phys. Lett. 94, 172101 (2009).

[5] W. Siemons *et al.*, Phys. Rev. B 81, 241308 (2010).

[6] C. Bell *et al.*, Phys. Rev. Lett. 103, 226802 (2009).